

Dynamic response characteristics of shallow-buried biased small clearance tunnel subjected to various ground shaking

Yanchao Li¹, Anmin Jiang², Yanchen Dong³, Feifei Wang⁴, Hanyang Guo⁵

^{1, 2, 3}Department of Management Engineering, Hunan Urban Construction College,

Xiangtan Hunan 411101, China

²School of Resource Environment and Safety Engineering, Hunan University of Science and Technology, Xiangtan, 411201, China

^{4, 5}School of Civil Engineering, Hunan City University, Yiyang Hunan, 413000, China

⁴Key Laboratory of Green Building and Intelligent Construction in Higher Educational Institutions of Hunan Province, Hunan City University, Yiyang, 413000, China

⁴Corresponding author

E-mail: ¹halesky@163.com, ²jianganmin123@126.com, ³2314061293@qq.com, ⁴1942016362@qq.com, ⁵321399806@qq.com

Received 29 October 2024; accepted 6 April 2025; published online 23 May 2025

DOI <https://doi.org/10.21595/jve.2025.24648>



Copyright © 2025 Yanchao Li, et al. This is an open access article distributed under the Creative Commons Attribution License, which permits unrestricted use, distribution, and reproduction in any medium, provided the original work is properly cited.

Abstract. The axial force and bending moment of tunnel lining are crucial for lining stability. To investigate the response patterns of axial force and bending moment in shallow-buried biased small clearance tunnels under various conditions – including different adjacent slope angles, loading wave types, peak loads, and loading directions – extensive numerical simulations were conducted. The numerical results were subsequently verified through large-scale vibration table physical model experiments. The findings reveal that the variation patterns of lining axial force and bending moment under bidirectional coupled seismic waves demonstrate similarity to those under vertical seismic waves. Vertical seismic motion exerts a more pronounced influence on lining axial force response. Seismic wave peak intensity significantly affects lining axial force and bending moment, with both parameters showing gradual increases corresponding to peak load escalation. The arch shoulder of the slope-side right tunnel lining exhibits particularly strong axial force and bending moment responses. While Darui wave, Wenchuan wave, and Kobe wave produce essentially consistent axial force and bending moment response patterns in tunnel linings, their magnitudes differ substantially. Seismic wave type primarily influences response magnitude rather than characteristic patterns of axial force distribution. Increasing slope angles adjacent to tunnels correlate with heightened axial force and bending moment responses in linings. A logarithmic functional relationship exists between slope angle and response values at the lining arch shoulder. These findings provide valuable references for seismic design of shallow-buried biased small clearance tunnels.

Keywords: tunnel engineering, various ground shaking, dynamic response, axial force, bending moment.

1. Introduction

Tunnels, as a form of transportation structure, have been widely used in highway transportation, railway transportation, and municipal transportation [1-3]. Due to various constraints on the selection of transportation routes, the shallow-buried biased small clearance tunnel is gradually being adopted [4-6]. The 2008 Wenchuan earthquake caused various forms of damage to a large number of tunnels. Scholars gradually realize the importance of seismic research on tunnels [7-8]. At present, the research on the seismic response law of shallow-buried biased small clearance tunnel is still not deep enough, and there is an urgent need to carry out relevant research work.

There are various research methods for studying the dynamic response law of tunnels,

including indoor physical model experiments [9-14], numerical simulation research methods [15-19], and theoretical calculation method for earthquake resistance [20-21] during recent years. Pan et al. [22] relied on a large-scale strike slip fault tunnel project to study the longitudinal distribution of tunnel structural response through model experiments and numerical simulations when crossing multiple rupture surfaces of strike slip faults. Huang et al. [23] used a high-precision indirect boundary integral equation method (IBIEM) to simulate the scattering effect of seismic waves on the overall model of mountain fault fracture zone tunnel. Three influencing factors were considered: incident wave intensity, distance between tunnel and fault fracture zone, and dynamic characteristics of fracture zone. The effects on the seismic dynamic response of mountain surface and tunnel were simulated. Xu et al. [24] established a three-dimensional train track tunnel soil coupled time-varying dynamic model to study the dynamic behavior of the train track tunnel soil interaction system under earthquake excitation. Different intensities of seismic waves and track irregularities were used as system excitation sources, and longitudinal, transverse, and vertical seismic waves were normalized through actual seismic records to analyze the dynamic response characteristics of the train track tunnel soil system under different soil conditions and earthquake intensities. Ma et al. [25] used a vibration table model test to obtain data information on the acceleration and dynamic strain of the test model under different intensities of seismic waves. Based on the macroscopic deformation characteristics of the experimental model, a multi-index evaluation method was adopted to reveal the regional spatial dynamic response characteristics of the tunnel damping structure. The plastic damping coefficient (PDC) of tunnel structures was defined based on the elastic-plastic effect, and the damage evolution law of tunnel structures is elucidated.

Currently, few studies have been conducted by scholars at home and abroad on the seismic response of shallow-buried biased small clearance tunnels. The dynamic response of such new tunnels (shallow-buried biased small clearance tunnel) is significantly different from that of conventional tunnels (non-biased tunnel, single tunnel). Numerical methods, as the most widely used scientific research method, have been utilized to study the dynamic response of tunnels. Based on the results of large-scale shaking table physical modeling tests that have been carried out in the acceleration response of tunnels, the results obtained by numerical methods are credible and reasonable through the comparison of shaking table tests and numerical methods. The tunnel lining axial force and bending moment cannot be obtained directly from the large-scale shaking table physical model test, but can be obtained by simulation based on reliable numerical simulation. The aim of this study is to rely on the results of large-scale shaking table physical model tests, and then to elaborate the response law of axial force and bending moment in shallow-buried biased small clearance tunnel through extended numerical parametric studies. This study investigates the effects of different parameters, including seismic wave type, seismic wave peak, seismic wave loading mode, and side slope angle, on the response of axial force and bending moment of tunnel lining. The research results can provide reference for seismic design of the shallow buried biased small clearance tunnels.

2. Numerical simulation

2.1. Engineering geology of tunnel

There are three types of rock types in the surrounding rock of the tunnel, from top to bottom: limestone, mudstone, and dolomite. Limestone is exposed on the surface and belongs to strongly weathered rock types. Mudstone has poor strength, while dolomite has good quality and stability. The rock mass surrounding the tunnel has low water content and no obvious groundwater. The maximum burial depth of the tunnel is 29 m, and one side of the tunnel is a natural slope with a slope angle of 60°. The closest distance between the slope and the tunnel is 13 m, and the overall stability of the slope is good. Through on-site engineering geological investigation, typical drill core samples were selected and indoor rock mechanics tests were conducted to obtain rock

mechanics parameters. Various engineering geological reduction methods were used to obtain rock mechanics parameters, and detailed mechanical parameters are shown in Table 1.

Table 1. Mechanical parameters of tunnel surrounding rock mass

Material	Bulk density γ (kN/m ³)	Elastic modulus E (MPa)	Cohesion c (kPa)	Internal friction angle φ (°)	Poisson's ratio μ
Dolomite	26.9	6956.5	1655.2	36.5	0.20
Mudstone	20.3	3561.2	613.5	30.1	0.26
Limestone	24.3	5360.2	961.3	32.7	0.21

2.2. Principles of finite element analysis

Structural dynamic time-range analysis is the process of calculating the structural response (displacements, velocities, internal forces) at any point in time when the structure is subjected to a dynamic load. The power balance equations used in MIDAS-GTS/NX dynamic time-range analysis are as follows:

$$[M]\ddot{u}(t) + [C]\dot{u}(t) + [K]u(t) = p(t), \quad (1)$$

where, $[M]$ is mass matrix, $[C]$ is damping matrix, $[K]$ is stiffness matrix, $p(t)$ is dynamic load (N), $\ddot{u}(t)$ is relative acceleration (m/s²), $\dot{u}(t)$ is relative speed (m/s), $u(t)$ is relative displacement (m).

The mode superposition method is used in the MIDAS-GTS/NX numerical simulation software for dynamic time history analysis of structures. The mode superposition method refers to the method of solving the displacement of a structure using a linear combination of mutually orthogonal displacement vectors, which has a significant effect on linear dynamic analysis of large structures. The prerequisite for using this method is that the damping matrix can be represented by a linear combination of mass matrix and stiffness matrix. This method can be represented by the following equation:

$$[C] = \alpha[M] + \beta[K], \quad (2)$$

$$\Phi^T M \Phi \ddot{q}(t) + \Phi^T C \Phi \dot{q}(t) + \Phi^T K \Phi q(t) = \Phi^T F(t), \quad (3)$$

$$m_i \ddot{q}_i(t) + c_i \dot{q}_i(t) + k_i q_i(t) = p_i(t), \quad (i = 1, 2, 3, \dots, m), \quad (4)$$

$$u(t) = \sum_{i=1}^m \Phi_i q_i(t), \quad (5)$$

$$q_i(t) = e^{-\xi_i \omega_i t} \left[q_i(0) \cos \omega_{Di} t + \frac{\xi_i \omega_i q_i(0) + \dot{q}_i(0)}{\omega_{Di}} \sin \omega_{Di} t \right] + \frac{1}{m_i \omega_{Di}} \int_0^t P_i(\tau) e^{-\xi_i \omega_i (t-\tau)} \sin \omega_{Di} (t-\tau) d\tau, \quad (6)$$

$$\omega_{Di} = \omega_i \sqrt{1 - \xi_i^2}, \quad (7)$$

where, α, β is Rayleigh coefficient, ξ_i is damping ratio of the i -th mode of vibration, ω_i is the natural period of the i -th mode of vibration, Φ_i is the shape of the i -th mode of vibration, $q_i(t)$ is solution of the i -th mode single degree of freedom equation.

The mode superposition method is one of the most commonly used methods in structural analysis programs. However, when the damping matrix cannot be represented as a linear combination of the mass matrix and the stiffness matrix, this method has certain limitations. This numerical simulation analysis adopts the mode superposition method to conduct dynamic time history response analysis of underground structures.

2.3. Numerical model for dynamic analysis

MIDAS-GTS/NX finite element analysis software is capable of transforming differential equations into linear algebraic equations for solving problems, and it is suitable for anisotropic, nonlinear, and nonuniform materials, and has effective applicability to complex boundary conditions. This finite element software can reveal the dynamic response law of tunnel lining under the loading of seismic wave. In this paper, the dynamic response of tunnel lining under seismic wave loading is analyzed using this finite element software. In order to avoid boundary effects in the numerical model, the model size is more than five times of the diameter of the tunnel lining [5]. Therefore, the length, width and height of the numerical model used in this numerical simulation study are 60 m, 40 m and 55 m, respectively.

The mesh type of the numerical model is quadrilateral mesh. The model calculation adopts the Mohr-Coulomb yield criterion. The bottom of the model boundary adopts a fixed boundary. The model is constrained in the X and Y directions. The top of the model has a free boundary. The Rayleigh damping coefficient is an important parameter for measuring the attenuation characteristics of structural vibration. The Rayleigh damping coefficient in this article is set to 0.03.

Kuhlemeyer and Lysmer [26] showed that for accurate representation of wave transmission through a model, the element size Δ_l , must be smaller than approximately 1/10 to 1/8 of the wave length associated with the highest frequency component of the input wave:

$$\Delta_l \leq \frac{\lambda}{10} \dots \frac{\lambda}{8} \quad (8)$$

where, λ is wave length of the propagated wave in the model. λ is related to the seismic wave velocity of micro-concrete (v_{mc}) and the highest frequency of the input motion (f_{max}) by the following relation:

$$\lambda = \frac{v_{mc}}{f_{max}} \quad (9)$$

Substituting Eq. (8) into Eq. (9) gives:

$$\Delta_l \leq \frac{v_{mc,min}}{10f_{max}} \quad (10)$$

According to the calculation results of Eqs. (8-10), the total number of nodes in the 3D tunnel lining calculation model is 10 263, and the total number of units is 56 125. The surrounding rock and lining in the numerical model are simulated by solid units, and the elastic-plastic intrinsic model and Mohr-Coulomb yield criterion are adopted. The specific calculation model is shown in Fig. 1.

2.4. Analysis scheme of numerical simulation

Three types of seismic waves are used for numerical simulation. The seismic waves are the Wenchuan (WC) wave, Darui (DR) wave and Kobe (KB) wave. The horizontal direction (X) is perpendicular to the tunnel axis, and vertical direction (Z) is perpendicular to table-board. Bidirectional coupled seismic waves are seismic waves that simultaneously load tunnels in two directions. Unidirectional seismic waves are seismic waves that load tunnels in only one direction. The acceleration time history curves of the seismic waves are shown in Fig. 2. The acceleration peaks of the seismic wave are adjusted to 0.4 g. The numerical simulation seismic wave loading scheme is shown in Table 2.

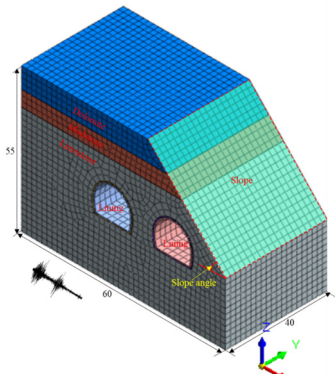


Fig. 1. Numerical calculation model (unit: m)

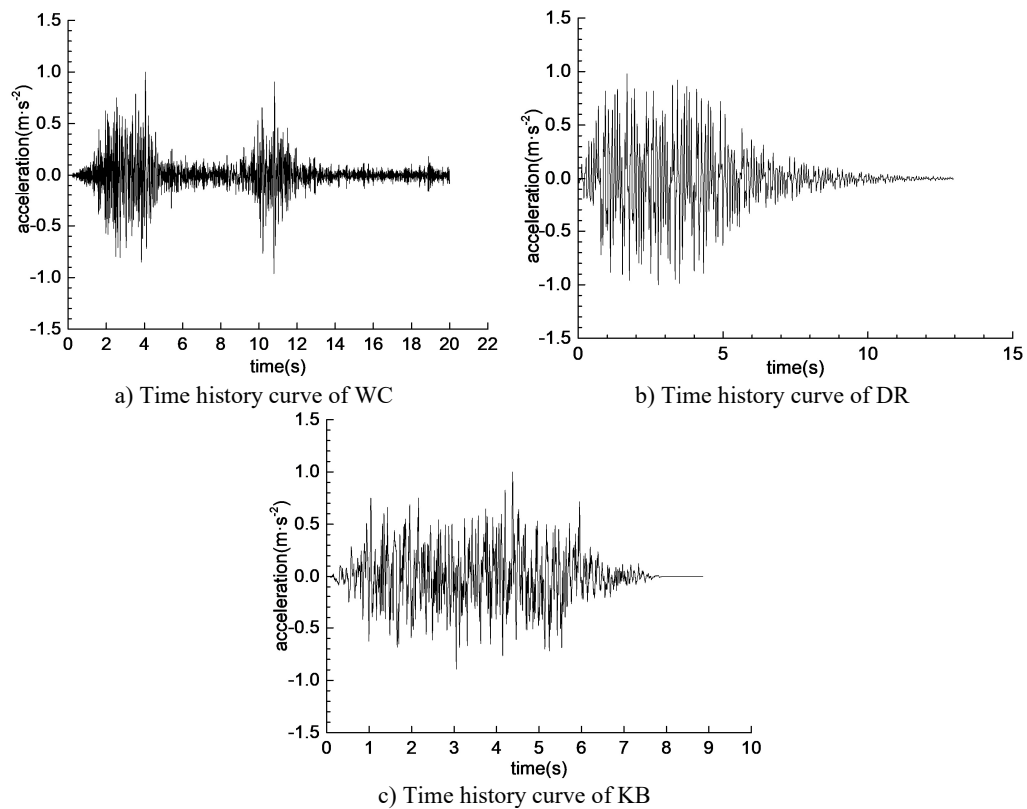


Fig. 2. Acceleration time-history curves of seismic wave

Table 2. Loading scheme of shaking table test

Number	seismic wave	Slope angle (°)	Loading direction	Load peak (m·s ⁻²)
1	DR	30	X	0.1, 0.2, 0.3, 0.4, 0.5, 0.6
2	DR	30	Z	
3	DR	30	XZ	
4	WC	30	XZ	
5	KB	30	XZ	
6	DR	45	X	
7	DR	60	X	
8	DR	90	X	

3. Analysis of calculation results

3.1. Verification of numerical simulation

In order to verify the reliability of the results of the study carried out by this numerical simulation, a series of physical model tests of a large-scale shaking table were carried out in the National Engineering Laboratory of High-Speed Railway Construction Technology of Central South University. The geometric similarity of the physical model is 1:10. Rigid model boxes were used in this shaker physical modeling test, which were made of steel plates, steel sections, and Plexiglas materials (Fig. 3). In order to eliminate the boundary effect of the model box, various energy-absorbing materials were attached inside the model box.

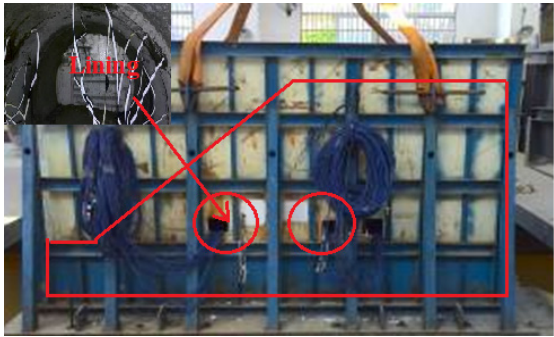


Fig. 3. Shaking table test

The lining model in the large vibrating table physical model test was made of micro-concrete. Reinforcing steel was simulated by galvanized iron wire. The thickness of the lining was 4 cm. The material ratio of the lining model was 1:6.9:1.3 (cement: sand: water). The compressive strength of the lining is 5 MPa. The surrounding rock of the tunnel is divided into three layers. The first layer is weakly weathered rock, the second layer is soft and weak rock, and the third layer is hard rock. The tunnel burial depth is 0.9 m, the net width of the tunnel is 0.7 m, and the thickness of the center partition wall is 0.4 m. After the physical model of the tunnel was completed, it was lifted onto the vibration table and tightly fixed. Firstly, white noise was loaded and the stability of the vibration table was verified. Then, the tunnel model was excited based on the seismic wave loading scheme.

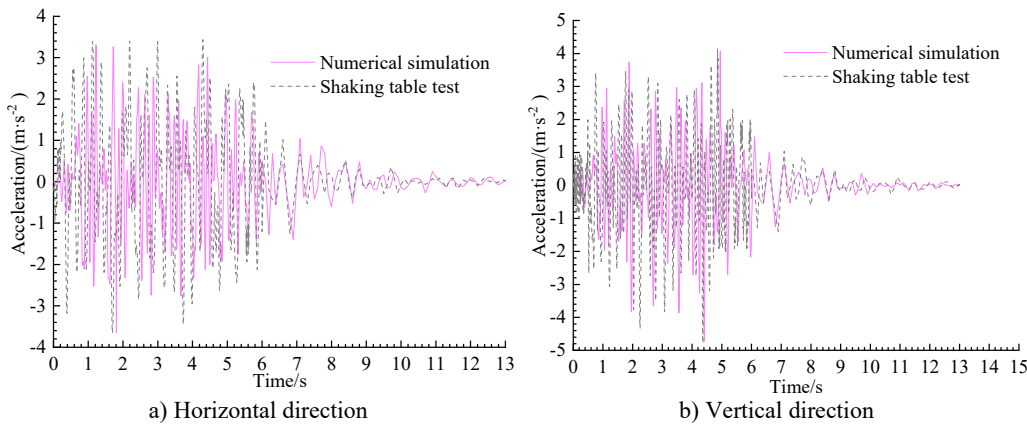


Fig. 4. Time-history curves of numerical simulation and shaking table test

The reliability of numerical simulation is verified by the acceleration response of tunnel. The

0.4 g Darui wave curve of shaking table test and numerical simulation are shown in Fig. 4. By comparing the results of numerical simulation and large-scale vibration table physical model experiments, the following conclusions can be drawn: (1) The acceleration response curves of the two research methods in the horizontal direction are similar and can match each other, and the peak acceleration response values are basically the same. The acceleration response curve in the horizontal direction has a strong response during the initial excitation stage. (2) The acceleration response curves of the two research methods in the vertical direction are similar and can be matched with each other, and the peak acceleration response values are basically the same. The acceleration response curve in the vertical direction shows a relatively stable response during the initial excitation stage and a severe response in the later stage. (3) The results of the two research methods are mutually validated, indicating that the numerical simulation results are in line with the laws of the physical model test results of large-scale vibration tables.

3.2. Lining dynamic axial force

The reliability of the numerical simulation results was verified through the use of a large-scale vibration table physical model experiment. Therefore, validated numerical models can be used to study the response patterns of various tunnels under seismic waves. According to the designed numerical simulation research plan, the axial force response laws of tunnel lining under slope angles of 30°, 45°, 60°, and 90° were revealed. The axial force response laws under the coupling direction conditions of X, Z, and XZ were revealed. The axial force response laws under the conditions of DR, WC and KB waves were revealed. The axial force response curves of tunnel lining are shown in Figs. 5-12.

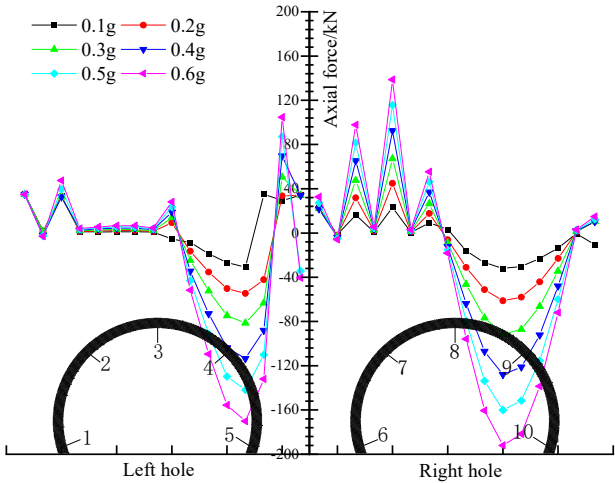


Fig. 5. Axial force of lining with DR-X and slope angle of 30°

According to Fig. 5, under the condition of a 30° slope angle, the axial force on the lining of a small clearance tunnel under the action of large horizontal waves shows a nonlinear trend. The axial force at the arch shoulders of the left and right tunnel lining is relatively large, and the maximum force at the right arch shoulder of the right tunnel near the slope is 190 kN. The axial force at the arch foot and arch top is relatively small, with a minimum of 5 kN. The peak load of seismic waves has an impact on the axial force of the lining, and as the excitation peak increases, the axial force gradually increases. The axial force response of the right tunnel lining near the slope surface is the strongest at the arch shoulder, mainly due to the small distance between the slope and the tunnel lining structure, which is greatly affected by seismic waves.

According to Fig. 6, under the condition of a 30° slope, the axial force of a small clearance

tunnel under the action of large vertical waves shows a nonlinear trend. The axial force is relatively large at the arch feet of the left and right holes, and the maximum axial force is 222 kN near the arch feet of the middle rock column. At the left arch crown and arch shoulder, the axial force at the right arch crown is the smallest, which is opposite to the trend under the action of large horizontal waves. The main reason is that under the action of vertical waves, the lining has an upward effect, and the arch foot generates a larger axial force under this effect. The axial force response of the right tunnel lining near the slope surface is strong at the arch shoulder, mainly due to the small distance between the slope and the tunnel lining structure, which is greatly affected by seismic waves.

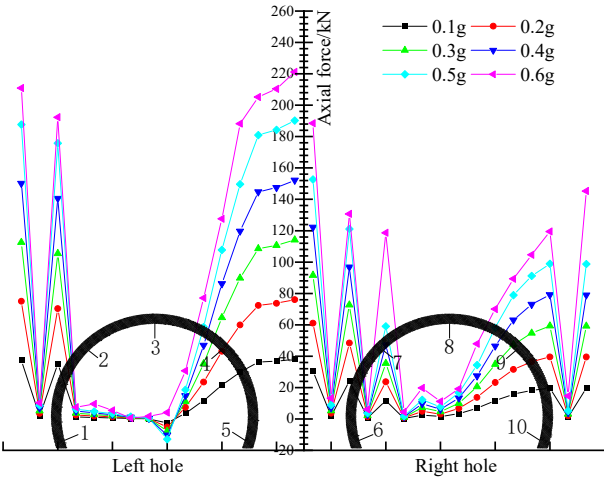


Fig. 6. Axial force of lining with DR-Z and slope angle of 30°

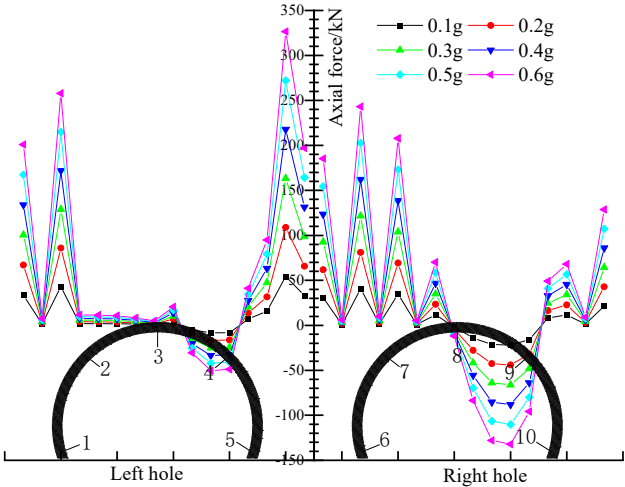


Fig. 7. Axial force of lining with DR-XZ and slope angle of 30°

From Fig. 7, under the condition of a 30° slope, the axial force of the small clearance tunnel lining shows a nonlinear trend under the action of coupled bidirectional large waves. The shear force is relatively high at the arch feet of the left and right holes, and the maximum shear force is 330kN near the arch feet of the middle rock column. The axial force response of the right tunnel lining near the slope surface is strong at the arch shoulder, mainly due to the small distance between the slope and the tunnel lining structure, which is greatly affected by seismic waves.

Under the bi-directional action of artificial seismic waves in Darui, the variation trend of lining axial force is similar to that of vertical axial force. This indicates that the vertical seismic action has a significant impact on the response of the lining axial force. The result of bidirectional coupling of Darui stronger than that of unidirectional seismic waves, indicating that the effect of bidirectional coupling is the most significant.

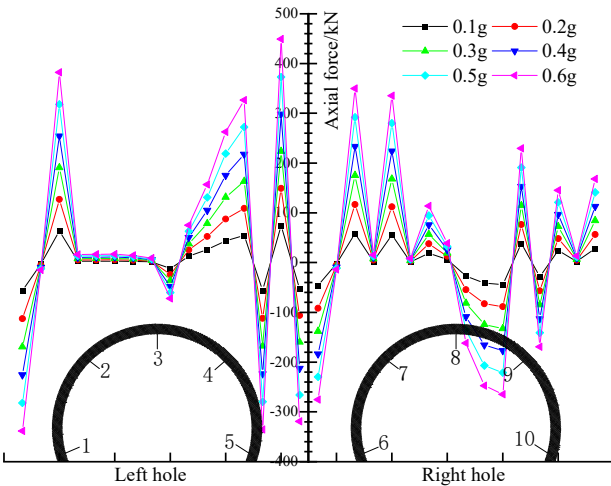


Fig. 8. Axial force of lining with WC-XZ and slope angle of 30°

According to Fig. 8, under the condition of a 30° slope, the axial force on the lining of a small clearance tunnel under the action of vertical Wenchuan wave shows a nonlinear trend. The axial force is relatively large at the arch feet of the left and right holes, and the maximum axial force is 445 kN near the arch feet of the middle rock column. Under the bi-directional action of the Wenchuan wave, the variation law of the axial force of the lining is similar to that of the Darui wave, except for the difference in the magnitude of the axial force. This indicates that the type of seismic wave has a relatively small impact on the response characteristics of the lining axial force, only affecting the numerical value of the lining axial force response.

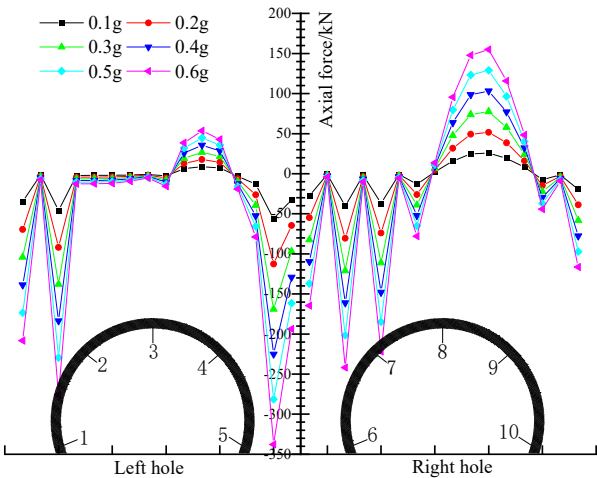


Fig. 9. Axial force of lining with KB-XZ and slope angle of 30°

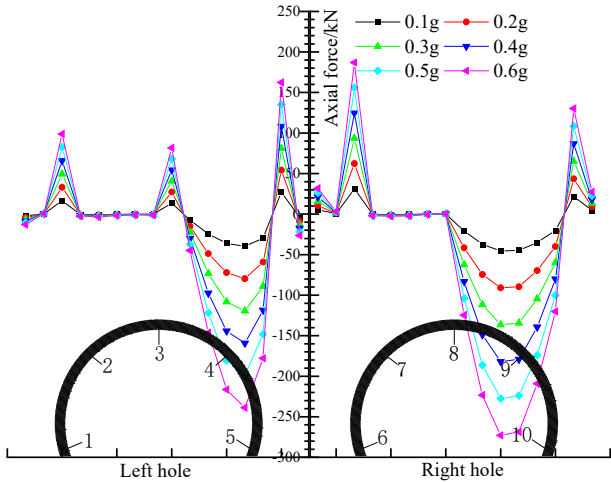


Fig. 10. Axial force of lining with DR-X and slope angle of 45°

According to Fig. 9, under the condition of a 30° slope, the lining of a small clearance tunnel exhibits a nonlinear trend under the action of horizontal Kobe wave. The maximum axial force at the arch foot of the left and right holes is 380 kN. The shear force at the shoulder and arch top of the left hole is relatively small. The peak load of seismic waves has an impact on the axial force of the lining, and as the peak load increases, the axial force gradually increases. The axial force response of the right tunnel lining near the slope surface is strong at the arch shoulder, mainly due to the small distance between the slope and the tunnel lining structure, which is greatly affected by seismic waves. By analyzing the axial force response laws of the lining under the action of Darui wave, Wenchuan wave, and Kobe wave, it can be concluded that the response laws under the three types of seismic waves are basically the same, except for the difference in the magnitude of the axial force. This indicates that the type of seismic wave has a relatively small impact on the response characteristics of the lining axial force, only affecting the numerical value of the lining axial force response.

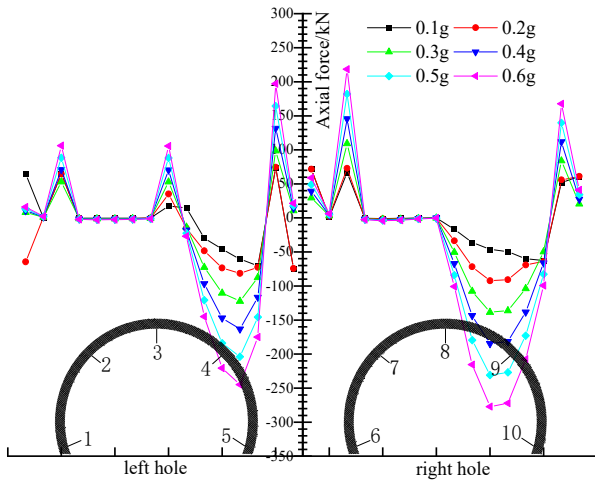


Fig. 11. Axial force of lining with DR-X and slope angle of 60°

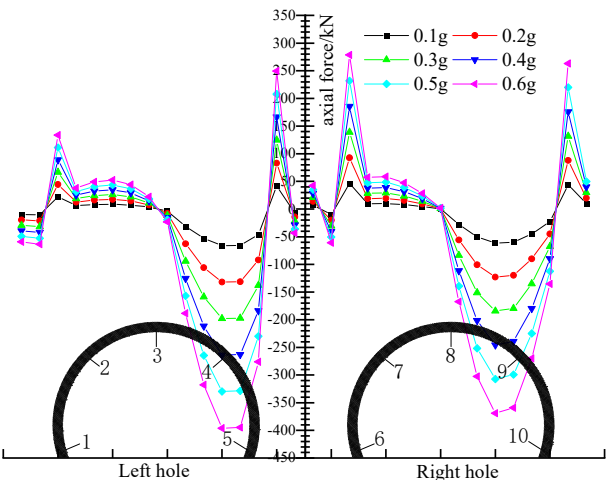


Fig. 12. Axial force of lining with DR-X and slope angle of 90°

From Fig. 10-12, the lining of small clearance tunnels exhibits a nonlinear trend under the action of large horizontal waves. The axial force response is maximum at the arch shoulder of the left tunnel near the middle partition wall and the arch shoulder of the right tunnel near the slope. The maximum axial force of the lining in the 30° slope angle model is 190 kN, the maximum axial force of the lining in the 45° slope angle model is 275 kN, the maximum axial force of the lining in the 60° slope angle model is 295 kN, and the maximum axial force of the lining in the 90° slope angle model is 370 kN (Table 3). From this, the axial force response of the lining arch shoulder near the slope increases with the increase of the slope angle, showing a nonlinear trend. The underlying mechanism behind the above pattern is the coupling effect between the adjacent slope structure and the lining structure. As the slope angle increases, the stability of the slope gradually decreases, and the potential sliding force inside the slope gradually increases. The potential sliding arc surface passes through the tunnel and exerts a shear effect on the tunnel lining structure. The larger the slope angle, the stronger the shear force on the tunnel lining. Therefore, the larger the slope angle, the stronger the coupling effect between the tunnel lining and the slope structure. The relationship between the slope angle and the axial force response value of the adjacent lining arch shoulder was fitted, and the fitting Eq. (11) was obtained. There is a logarithmic function relationship between the slope angle and the axial force response of the lining arch shoulder:

$$y = 157.79\ln(x) - 340.85, \quad (11)$$
$$R^2 = 0.9775,$$

where, x is slope angle, ° (0°-90°); y is maximum axial force for lining, kN.

Table 3. Maximum axial force of the lining

Slope angle (°)	Maximum axial force for lining (kN)
30	190
45	275
60	295
90	370

3.3. Lining dynamic bending moment

The reliability of the numerical simulation results was verified through the use of a large-scale vibration table physical model experiment. Therefore, validated numerical models can be used to study the response patterns of various tunnels under seismic waves. According to the designed

numerical simulation research plan, the bending moment response laws of tunnel lining under slope angles of 30°, 45°, 60°, and 90° were revealed. The bending moment response laws under the coupling direction conditions of X, Z, and XZ were revealed. The bending moment response laws under the conditions of DR, WC and KB waves were revealed. The bending moment response curves of tunnel lining are shown in Figs. 14-19.

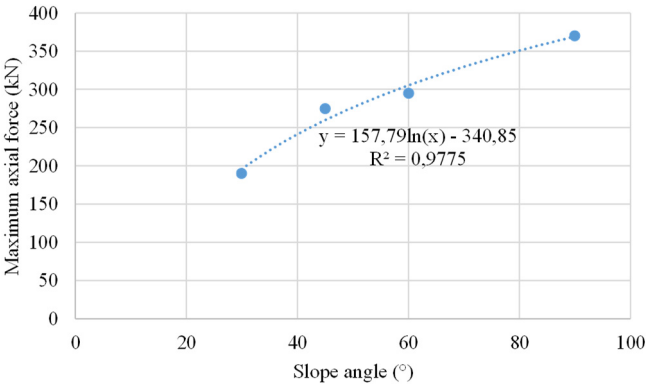


Fig. 13. Curve of axial force fitting for tunnel lining

From Fig. 14, under the condition of a 30° slope, the bending moment of the lining of a small clearance tunnel under the action of a large vertical rake shows a nonlinear trend. The bending moment is relatively large at the arch foot of the left and right tunnels, and the axial force of the right tunnel is the highest near the arch foot of the middle rock column, with a maximum of 6 kN·m. The peak load of seismic waves has an impact on the bending moment of the lining, and as the excitation peak increases, the bending moment gradually increases. The bending moment response of the right tunnel lining near the slope surface is relatively strong at the arch shoulder, mainly due to the small distance between the slope and the tunnel lining structure, which is greatly affected by seismic waves.

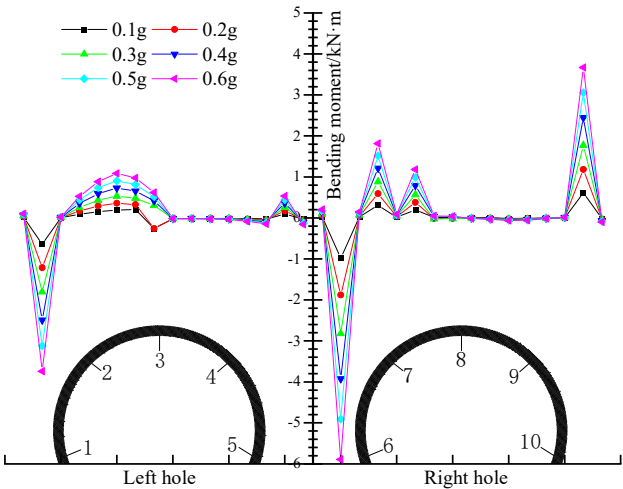


Fig. 14. Bending moment of lining with DR-X and slope angle of 30°

According to Fig. 15, under the condition of a 30° slope, the bending moment of the lining of a small clearance tunnel under the action of bidirectional coupled Darui wave shows a nonlinear trend. The bending moment is relatively large at the arch foot of the left and right holes, and the axial force of the right hole is the highest near the arch foot of the middle rock column, with a

maximum of 6.8 kN·m. The peak load of seismic waves has an impact on the bending moment of the lining, and as the excitation peak increases, the bending moment gradually increases. The right tunnel lining near the slope surface has the strongest bending moment response at the arch shoulder, reaching a bending moment of 8 kN·m. Mainly due to the small distance between the slope and the tunnel lining structure, it is greatly affected by seismic waves.

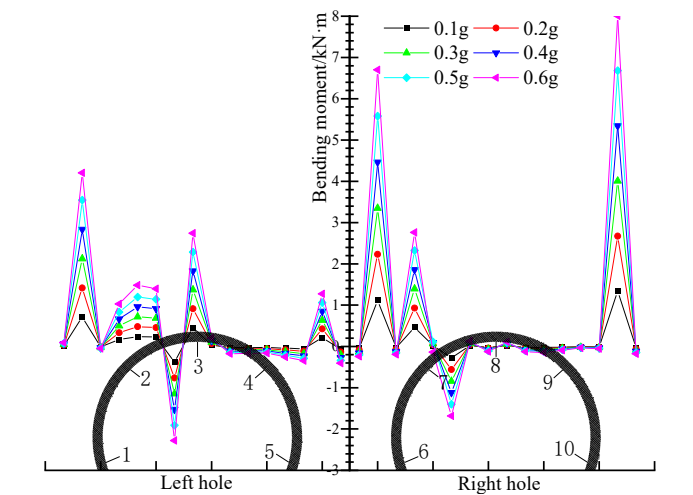


Fig. 15. Bending moment of lining with WC-XZ and slope angle of 30°

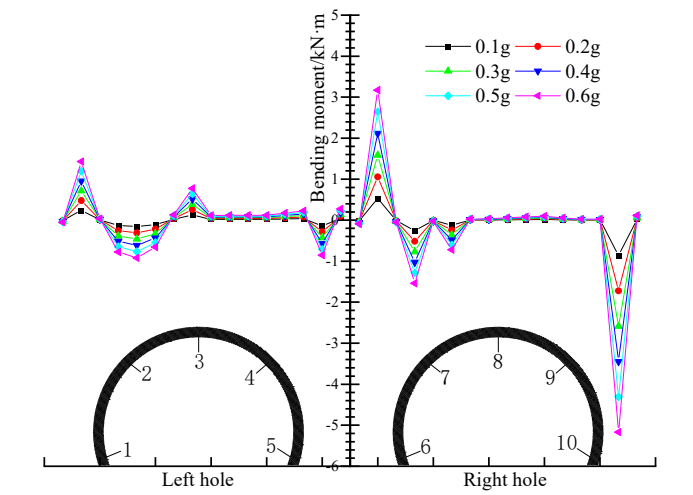


Fig. 16. Bending moment of lining with KB-XZ and slope angle of 30°

As shown in Fig. 16, under the condition of a 30° slope, the bending moment of the lining of a small clearance tunnel under the action of bidirectional coupled Kobe wave exhibits a nonlinear trend. The bending moment is relatively large at the arch foot of the left and right holes, and the axial force of the right hole is the highest near the arch foot of the middle rock column, with a maximum of 3.1 kN·m. The peak load of seismic waves has an impact on the bending moment of the lining, and as the excitation peak increases, the bending moment gradually increases. The right tunnel lining near the slope surface has the strongest bending moment response at the arch shoulder, with a bending moment of 5.2 kN·m. Mainly due to the small distance between the slope and the tunnel lining structure, it is greatly affected by seismic waves. The results of bidirectional coupled Kobe wave are weaker than those of large Rayleigh waves, indicating that the type of

seismic wave has an impact on the magnitude of the lining bending moment. By analyzing the bending moment response laws of the lining under the action of Darui wave, Wenchuan wave, and Kobe wave, it can be concluded that the response laws under the three types of seismic waves are basically the same, except for the difference in the magnitude of the bending moment. This indicates that the type of seismic wave has a relatively small impact on the response characteristics of the lining bending moment, only affecting the numerical value of the lining bending moment response.

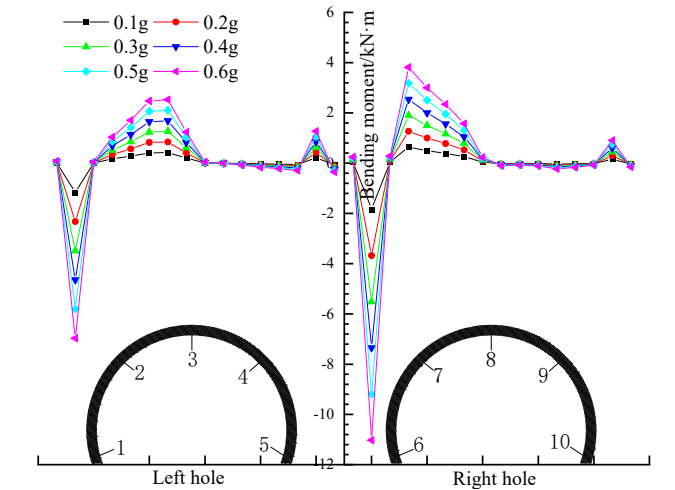


Fig. 17. Bending moment of lining with DR-X and slope angle of 45°

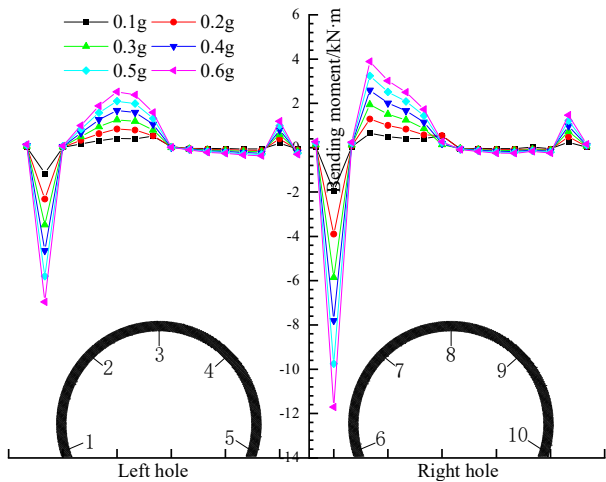


Fig. 18. Bending moment of lining with DR-X and slope angle of 60°

From Figs. 17-19, the lining of small clearance tunnels exhibits a nonlinear trend under the action of large horizontal waves. The bending moment response is maximum at the arch shoulder and arch foot near the middle partition wall of the right tunnel. The maximum bending moment of the lining in the 30° slope angle model is 6 kN·m, in the 45° slope angle model it is 11 kN·m, in the 60° slope angle model it is 12 kN·m, and in the 90° slope angle model it is 16 kN·m (Table 4). From this, it can be seen that the bending moment response of the lining arch foot increases with the increase of the slope angle, showing a nonlinear trend of change. The underlying mechanism behind the above pattern is the coupling effect between the adjacent slope structure

and the lining structure. As the slope angle increases, the stability of the slope gradually decreases, and the potential sliding force inside the slope gradually increases. The potential sliding arc surface passes through the tunnel and exerts a shear effect on the tunnel lining structure. The larger the slope angle, the stronger the shear force on the tunnel lining. Therefore, the larger the slope angle, the stronger the coupling effect between the tunnel lining and the slope structure. The relationship between the slope angle and the bending moment response value of the lining arch shoulder was fitted, and the fitting Eq. (12) was obtained. There is a logarithmic function relationship between the slope angle and the bending moment response of the lining arch shoulder:

$$y = 8.74\ln(x) - 23.28, \quad (12)$$
$$R^2 = 0.9709,$$

where, x is slope angle, $^{\circ}$ (0° - 90°); y is maximum bending moment of lining, $\text{kN}\cdot\text{m}$.

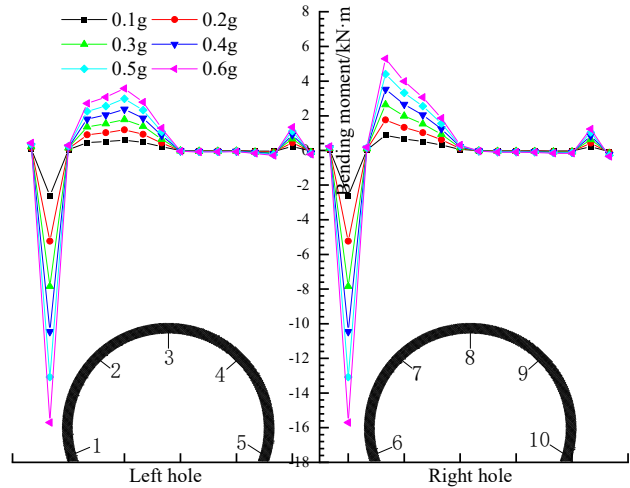


Fig. 19. Bending moment of lining with DR-X and slope angle of 90°

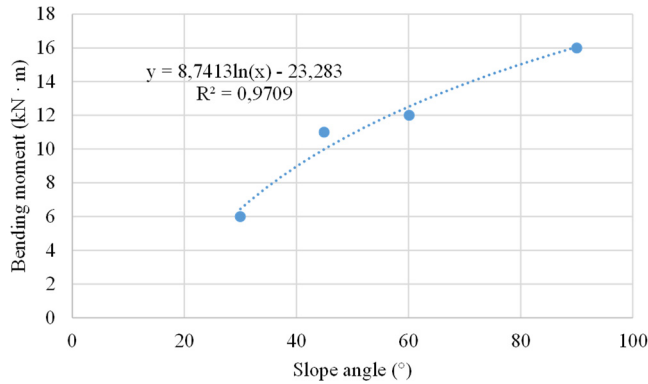


Fig. 20. Curve of bending moment fitting for tunnel lining

The article analyzed the magnitude of axial force and bending moment of tunnel lining under different slope angles. The axial force and bending moment of tunnel lining vary greatly at different angles. The influence of slope angle on the axial force and bending moment of tunnel lining is significant. And the fitting formula was obtained by using the fitting analysis method. The axial force and bending moment of tunnel lining at any slope angle can be calculated by fitting the formula.

Table 4. Maximum bending moment of the lining

Slope angle (°)	Maximum bending moment for lining (kN·m)
30	6
45	11
60	12
90	16

4. Conclusions

The response laws of axial force and bending moment of shallow buried biased small clearance tunnels under different adjacent slope angles, different loading wave types, different loading peaks, and different loading directions were studied using numerical simulation methods. The following conclusions were obtained:

1) Under the action of bidirectional coupled seismic waves, the variation trend of lining axial force and bending moment is similar to that of vertical axial force, and the response strength is greater than that of unidirectional seismic waves. The vertical seismic action has a significant impact on the response of lining axial force.

2) The peak load of seismic waves has an impact on the axial force and bending moment of the lining, and as the peak load increases, the axial force and bending moment gradually increase. The right tunnel lining near the slope surface has a strong axial force and bending moment response at the arch shoulder.

3) Under the action of three types of seismic waves, the axial force and bending moment response laws of tunnel lining are basically the same, except for the differences in the magnitude of axial force and bending moment. The type of seismic wave has little effect on the response characteristics of lining axial force, only affecting the numerical value of lining axial force response.

4) As the angle of the slope near the tunnel increases, the axial force and bending moment response values of the tunnel lining also increase. There is a logarithmic function relationship between the slope angle and the axial force and bending moment response values of the lining arch shoulder.

5) The dynamic response law of the tunnel was studied using physical model experiments and numerical simulations. Further research is needed on the theory of dynamics.

Acknowledgements

This work was supported by the Natural Sciences Funding Project of Hunan Province (2024JJ6110, 2024JJ8049), Application Basic Research and Soft Science Research Plan of Yiyang City (2024YR02), and aid program for Science and Technology Innovative Research Team in Higher Educational Institutions of Hunan Province.

Data availability

The datasets generated during and/or analyzed during the current study are available from the corresponding author on reasonable request.

Author contributions

Yanchao Li and Feifei Wang wrote the initial draft of the paper. Anmin Jiang and Feifei Wang conducted physical model tests on the vibration table. Hanyang Guo conducted numerical simulation analysis. Yanchao Li and Yanchen Dong reviews the manuscript of the paper.

Conflict of interest

The authors declare that they have no conflict of interest.

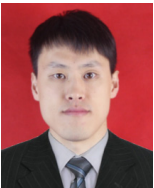
References

- [1] W. L. Wang, T. T. Wang, J. J. Su, C. H. Lin, C. R. Seng, and T. H. Huang, "Assessment of damage in mountain tunnels due to the Taiwan Chi-Chi earthquake," *Tunnelling and Underground Space Technology*, Vol. 16, No. 3, pp. 133–150, Jul. 2001, [https://doi.org/10.1016/s0886-7798\(01\)00047-5](https://doi.org/10.1016/s0886-7798(01)00047-5)
- [2] Y. M. A. Hashash, J. J. Hook, B. Schmidt, and J. I.-Chiang Yao, "Seismic design and analysis of underground structures," *Tunnelling and Underground Space Technology*, Vol. 16, No. 4, pp. 247–293, Oct. 2001, [https://doi.org/10.1016/s0886-7798\(01\)00051-7](https://doi.org/10.1016/s0886-7798(01)00051-7)
- [3] Q. Gao, *The Memoir on Tunnel and Underground Structure of Gao Quqing*. Beijing: China Railway Publishing House, 1996.
- [4] X. L. Jiang et al., "Dynamic response of shallow-buried tunnels under asymmetrical pressure distributions," *Journal of Testing and Evaluation*, Vol. 46, No. 4, pp. 1574–1590, Jul. 2018, <https://doi.org/10.1520/jte20170026>
- [5] X. Jiang, F. Wang, H. Yang, G. Sun, and J. Niu, "Dynamic response of shallow-buried small spacing tunnel with asymmetrical pressure: shaking table testing and numerical simulation," *Geotechnical and Geological Engineering*, Vol. 36, No. 4, pp. 2037–2055, Jan. 2018, <https://doi.org/10.1007/s10706-017-0444-0>
- [6] F. Wang, X. Jiang, and J. Niu, "The large-scale shaking table model test of the shallow-bias tunnel with a small clear distance," *Geotechnical and Geological Engineering*, Vol. 35, No. 3, pp. 1093–1110, Jan. 2017, <https://doi.org/10.1007/s10706-017-0166-3>
- [7] Y. Jiang, C. Wang, and X. Zhao, "Damage assessment of tunnels caused by the 2004 Mid Niigata Prefecture Earthquake using Hayashi's quantification theory type II," *Natural Hazards*, Vol. 53, No. 3, pp. 425–441, Sep. 2009, <https://doi.org/10.1007/s11069-009-9441-9>
- [8] Z. Z. Wang and Z. Zhang, "Seismic damage classification and risk assessment of mountain tunnels with a validation for the 2008 Wenchuan earthquake," *Soil Dynamics and Earthquake Engineering*, Vol. 45, No. 2, pp. 45–55, Feb. 2013, <https://doi.org/10.1016/j.soildyn.2012.11.002>
- [9] G. Tsinidis, K. Pitilakis, G. Madabhushi, and C. Heron, "Dynamic response of flexible square tunnels: centrifuge testing and validation of existing design methodologies," *Geotechnical Earthquake Engineering*, Vol. 65, No. 5, pp. 71–87, Dec. 2015, <https://doi.org/10.1680/gee.61491.071>
- [10] G. Tsinidis, K. Pitilakis, and G. Madabhushi, "On the dynamic response of square tunnels in sand," *Engineering Structures*, Vol. 125, pp. 419–437, Oct. 2016, <https://doi.org/10.1016/j.engstruct.2016.07.014>
- [11] G. Tsinidis, E. Rovithis, and K. Pitilakis, "Seismic response of boxtype tunnels in soft soil: experimental and numerical investigation," *Tunnelling and Underground Space Technology*, Vol. 9, pp. 199–214, 2016.
- [12] O. Abuhajar, H. El Naggar, and T. Newson, "Seismic soil-culvert interaction," *Canadian Geotechnical Journal*, Vol. 52, pp. 1–19, 2015.
- [13] O. Abuhajar, H. El Naggar, and T. Newson, "Experimental and numerical investigations of the effect of buried box culverts on earthquake excitation," *Soil Dynamics and Earthquake Engineering*, Vol. 79, pp. 130–148, Dec. 2015, <https://doi.org/10.1016/j.soildyn.2015.07.015>
- [14] A. Hushmand, S. Dashti, C. Davis, J. S. McCartney, and B. Hushmand, "A centrifuge study of the influence of site response, relative stiffness, and kinematic constraints on the seismic performance of buried reservoir structures," *Soil Dynamics and Earthquake Engineering*, Vol. 88, pp. 427–438, Sep. 2016, <https://doi.org/10.1016/j.soildyn.2016.06.011>
- [15] S. Kontoe, L. Zdravkovic, D. M. Potts, and C. O. Menkiti, "On the relative merits of simple and advanced constitutive models in dynamic analysis of tunnels," *Géotechnique*, Vol. 61, No. 10, pp. 815–829, Oct. 2011, <https://doi.org/10.1680/geot.9.p.141>
- [16] S. Kontoe, V. Avgerinos, and D. M. Potts, "Numerical validation of analytical solutions and their use for equivalent-linear seismic analysis of circular tunnels," *Soil Dynamics and Earthquake Engineering*, Vol. 66, pp. 206–219, Nov. 2014, <https://doi.org/10.1016/j.soildyn.2014.07.004>
- [17] E. Bilotta, G. Lanzano, S. P. G. Madabhushi, and F. Silvestri, "A numerical Round Robin on tunnels under seismic actions," *Acta Geotechnica*, Vol. 9, No. 4, pp. 563–579, May 2014, <https://doi.org/10.1007/s11440-014-0330-3>

- [18] G. Lanzano, E. Bilotta, G. Russo, F. Silvestri, and S. P. G. Madabhushi, "Centrifuge modeling of seismic loading on tunnels in sand," *Geotechnical Testing Journal*, Vol. 35, No. 6, pp. 1–16, Nov. 2012, <https://doi.org/10.1520/gtj104348>
- [19] G. Lanzano, E. Bilotta, G. Russo, and F. Silvestri, "Experimental and numerical study on circular tunnels under seismic loading," *European Journal of Environmental and Civil Engineering*, Vol. 19, No. 5, pp. 539–563, May 2015, <https://doi.org/10.1080/19648189.2014.893211>
- [20] S. K., K. I. Praseeda, and C. Pany, "Moderating the soft storey impact in multi-storey buildings: A comparative seismic investigation," *Journal of Sustainable Construction Materials and Technologies*, Vol. 9, No. 4, pp. 355–364, Dec. 2024, <https://doi.org/10.47481/jscmt.1607472>
- [21] C. Pany and G. Li, "Editorial: Application of periodic structure theory with finite element approach," *Frontiers in Mechanical Engineering*, Vol. 9, Apr. 2023, <https://doi.org/10.3389/fmech.2023.1192657>
- [22] X. Pan, Y. Shen, and H. Wang, "Study on response characteristics of the tunnel structure under dislocation of strike-slip faults with multiple fracture surfaces," *Modern Tunnelling Technology*, Vol. 61, No. 4, pp. 210–220, Apr. 2024.
- [23] L. Huang, Y. Zhou, and Z. Liu, "Analysis of the interaction between mountains-fault zones-tunnels under SH wave incidence," *Journal of Disaster Prevention and Mitigation Engineering*, Vol. 44, No. 4, pp. 870–880, Apr. 2024.
- [24] L. Xu, X. Wang, and Z. Yu, "Dynamic analysis of train-track-tunnel-soil interaction system under seismic excitation," *Journal of Central South University (Science and Technology)*, Vol. 55, No. 6, pp. 2359–2369, Jun. 2024.
- [25] Z. Ma, H. Wu, and Z. Yi, "Experimental study on the evaluation method of damping effect of linings in tunnel crossing landslides in high-intensity seismic zone," *China Earthquake Engineering Journal*, Vol. 46, No. 5, pp. 1084–1096, May 2024.
- [26] R. L. Kuhlemeyer and J. Lysmer, "Finite element method accuracy for wave propagation problems," *Journal of the Soil Mechanics and Foundations Division*, Vol. 99, No. 5, pp. 421–427, May 1973, <https://doi.org/10.1061/jsfeaq.0001885>



Yanchao Li have received M.S. degree in Central South University, Changsha, China, in 2013. At present, he is a part-time teacher in the Department of Management Engineering of Hunan Urban Construction College.



Anmin Jiang obtained a Master's degree from Central South University of Forestry and Technology in Changsha, China, in 2015. At present, he is currently a full-time teacher in the Department of Management Engineering at Hunan Urban Construction College.



Yanchen Dong obtained a Master's degree from Central South University of Forestry and Technology in Changsha, China, in 2017. At present, she is currently a full-time teacher in the Department of Management Engineering at Hunan Urban Construction College.



Feifei Wang received M.S. degree in Central South University of Forestry and Technology, Changsha, China, in 2018. His current research interests include slope engineering and rock mechanics. He is currently studying for a Ph.D. at Chongqing Jiaotong University.



Hanyang Guo is currently studying in the Department of Water Resources and Hydropower Engineering at Hunan City University with a Bachelor's degree, mainly focusing on the management of water resources and hydropower projects.